DOI 10.1007/s11041-023-00947-6
Metal Science and Heat Treatment, Vol. 65, Nos. 7 – 8, November, 2023 (Russian Original Nos. 7 – 8, July – August, 2023)

STRUCTURAL STEELS

UDC 669.018.298:620.17:620.18

FORMATION OF STRUCTURE AND PROPERTIES OF LOW-CARBON BAINITE IN STEEL 08KhFA

M. A. Vyboishchik,[1] I. V. Gruzkov,[1] E. A. Chistopol'tseva,[2] and T. V. Tetyueva[2]

Translated from *Metallovedenie i Termicheskaya Obrabotka Metallov*, No. 7, pp. 8 – 16, July, 2023.

Original article submitted February 1, 2023.

The structure, mechanical properties and corrosion resistance of steel 08KhFA are studied after tempering at different temperatures. The succession of the structural changes and the temperature ranges of the phase and structural transformations occurring in tempering of lath, carbide-free and low-carbon bainite are determined. The structural features of lath bainite in steel 08KhFA, the process modes providing its formation, and the combination of high strength properties with corrosion resistance under oilfield operating conditions are presented.

Key words: oilfield environment, pipe steels, strength, ductility, corrosion resistance, structural state, ferrite, bainite.

INTRODUCTION

Progressive enhancement of the aggressive action of oilfield environments with increasing carbon dioxide corrosion and intensification of oil production demands enhancement of the corrosion resistance of the oil producing equipment. In the recent years, carbon steels have been replaced by low-carbon low-alloy steels with bainitic hardenability, which has raised the operating capacity of the pipes [1, 2]. However, the rate of failure of the oil production pipes is still much higher than it is permissible [3]. It is important to raise the resistance of low-alloy steels to corrosion and mechanical fracture in the production of oil.

It is obvious that a bainitic structure providing a unique combination of high strength and ductility will remain the basic structural state for both available and novel pipe steels for a long time. The task to raise the corrosion resistance of steels with bainitic structure in aggressive oil production environments awaits solution. The mechanical properties of such steels and the formation of bainitic structures in them have been described in the relevant literature well enough [2, 4 – 10]. At the same time, the relation between the morphology of the bainitic structure and the resistance of the steels to corrosion and mechanical fracture remains virtually unstudied.

The aim of the present work was to study the relation between the structure of low-carbon bainite and the mechanical properties and corrosion behavior of steel 08KhFA in oilfield environments.

METHODS OF STUDY

We studied steel 08KhFA with composition (in wt.%) 0.09 C, 0.52 Cr, 0.44 Mn, 0.20 Si, 0.012 Ni, 0.11 Cu, 0.088 V, 0.02 Nb, 0.003 Mo, 0.002 Sm 0.011 P. This matches the widely used grade 13KhFA except for the lower carbon content (0.05 – 0.09 wt.%). The reduced carbon content eliminates the peritectic transformation of the steel under crystallization and thus lowers the probability of formation of hot cracks and raises the corrosion resistance.

To determine the relation between the structure and the properties of the steel we resorted to the research methods describing the structural condition and the operating properties corresponding to this condition.

We performed the following studies.

[1] Tolyatti State University, Tolyatti, Russia.
[2] "IT-Service" Company, Samara, Russia (e-mail: gigabon7@mail.ru).

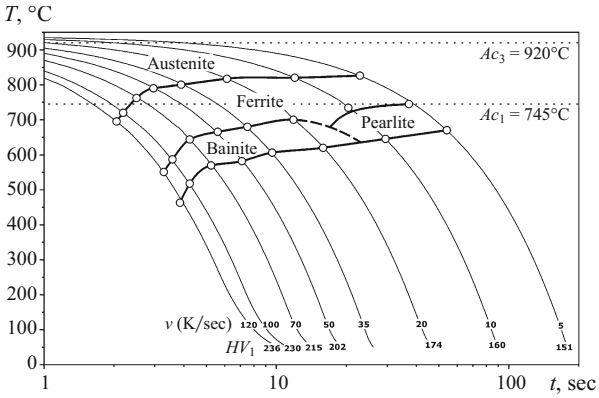

Fig. 1. Thermokinetic diagram of decomposition of supercooled austenite in steel 08KhFA.

1. Metallographic analysis involving optical microscopy (GX51 microscope of the Olympus Company), scanning electron microscopy (XL-30 microscope of the Philips Company), transmission electron microscopy (UMV-100L microscope), diffraction analysis, and EBSD with determination of the angles of misorientation between grains.

2. X-ray diffraction analysis for determining the volume fraction of phases and the stress state (the residual stresses of the third kind and the dislocation density) with the help of a Shimadzu Maxima XRD-7000S diffractometer (copper K_α radiation, tube power 1.6 kW) in angle range $2\theta = 40 – 100°$. The crystalline phases were identified using the Shimadzu PDF2 database. The full-profile analysis of the diffraction patterns was performed by the methods of Le Bail and Rietveld using the Jana2006 software.

3. Determination of the dissipation of the supplied energy by the method of internal friction in terms of the heights of the Snoek and Snoek–Koster relaxation peaks and of the concentration of carbon atoms in the solid solution and on dislocations.[3]

4. Assessment of mechanical properties in tests for uniaxial tension (GOST 1497) and impact toughness (GOST 9454) and hardness measurements (GOST 9013).

5. Determination of the resistance of the steel to corrosion fracture in tests for hydrogen cracking (NACE TM0284), for sulfide stress corrosion cracking (NACE TM0177), and for resistance to carbon dioxide corrosion.

The carbon dioxide corrosion was simulated by the method developed by the “IT-Service” Company (a hold for 400 h in an aggressive medium, i.e., 3.5% chloride at 65°C and carbon dioxide CO_2 at a pressure of 0.1 MPa), which allowed us to create on the surface of the sample corrosion products similar to those formed under field conditions after many-months’ service in carbon dioxide oilfield environments.

To assess the effect of the temperature and of the cooling rate on the structure of steel 08KhFA, we plotted the thermokinetic diagram of the transformation of austenite (Fig. 1) and used the method of end quenching (GOST 5657) with panoramic imaging of variation of the structure over the length of an end sample (Fig. 2).

[3] The data were measured and processed at the Tula State Pedagogical University in the laboratory of mechanical spectroscopy under the guidance of Professor A. N. Chukanov.

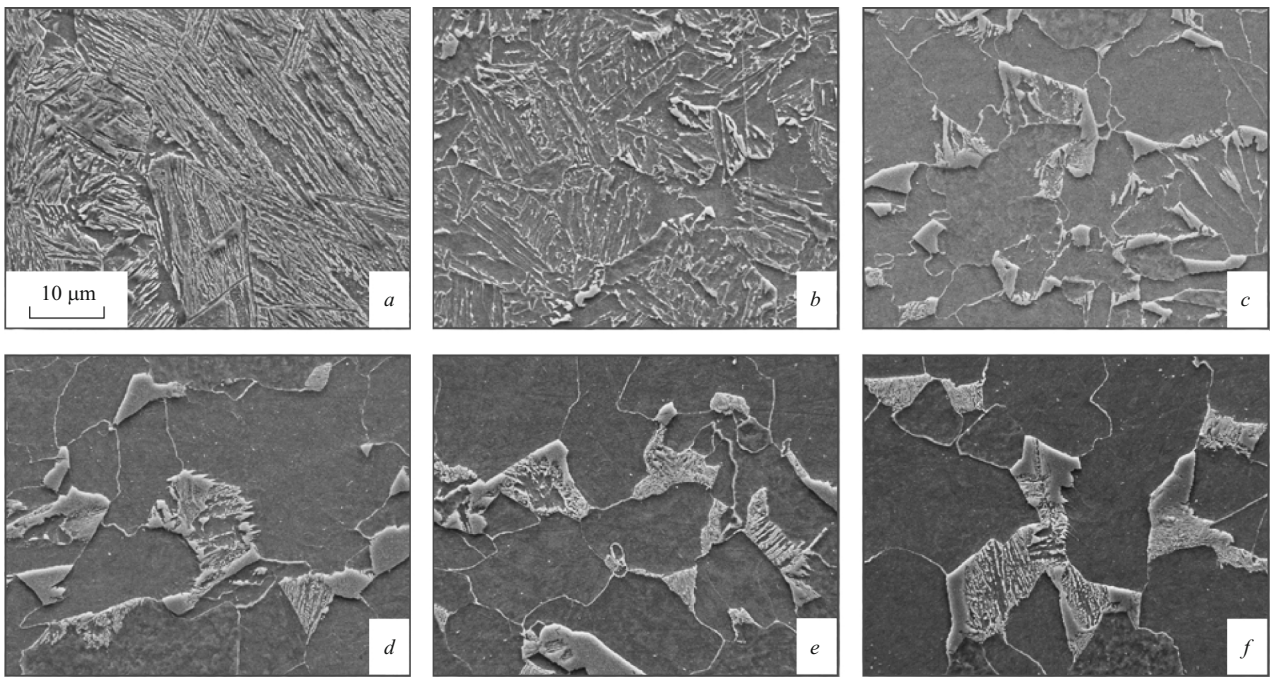

Fig. 2. Structure of steel 08KhFA after end quenching: *a*) at distance $h = 2$ mm from the end of the sample, hardness 310 *HV*; *b*) $h = 7$ mm, 231 *HV*; *c*) $h = 12$ mm, 182 *HV*; *d*) $h = 17$ mm, 163 *HV*; *e*) $h = 22$ mm, 155 *HV*; *f*) $h = 27$ mm, 152 *HV*.

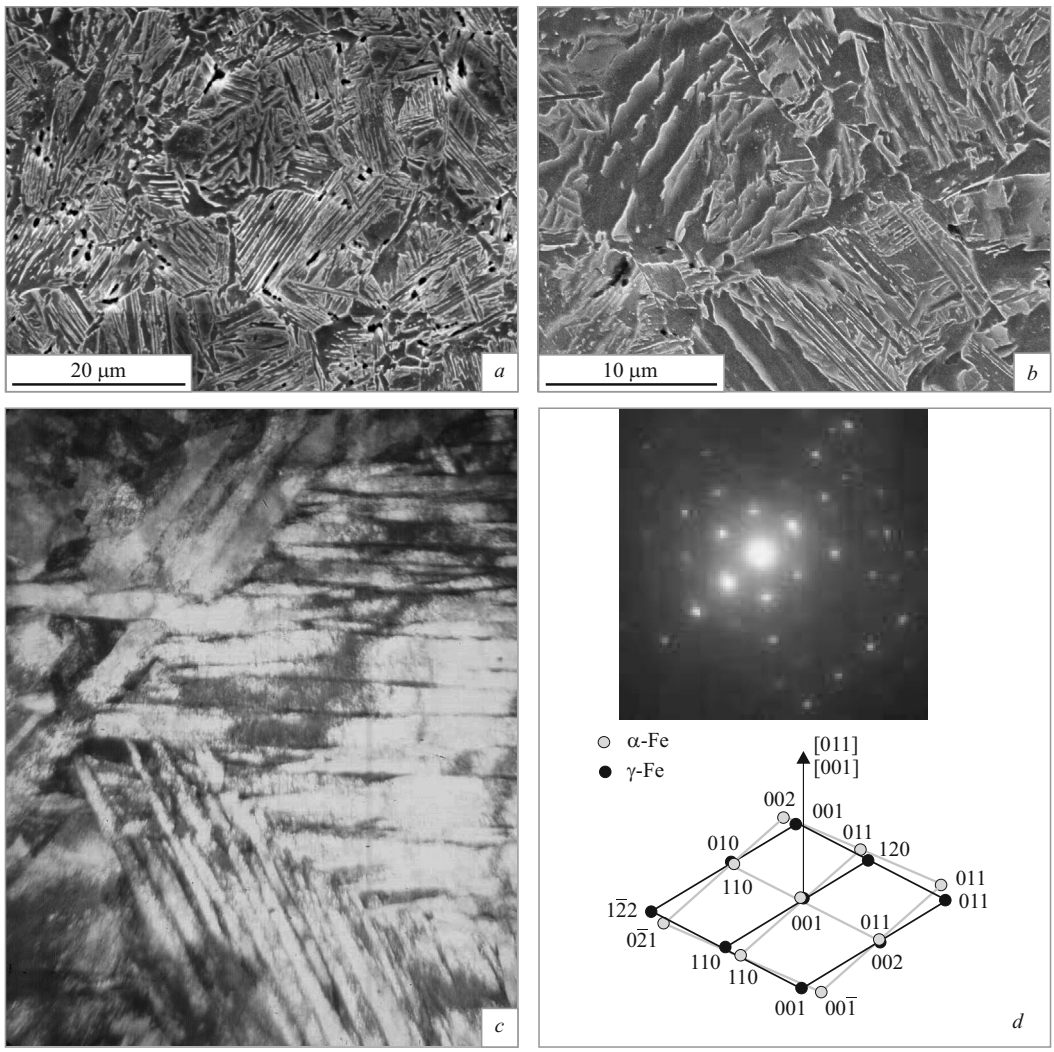

Fig. 3. Structure of steel 08KhFA after water quenching from 930°C: *a*, *b*) scanning electron microscopy; *c*) transmission electron microscopy (light background, × 11,000); *d*) microdiffraction.

RESULTS

It can be seen from the thermokinetic diagram of decomposition of supercooled austenite (Fig. 2) that bainite forms in the steel in a wide range of cooling rates (up to 15 K/sec) and has peculiar structural features.

To provide a relatively homogeneous and identical structural state, all the samples were subjected to 30-min normalizing at 940°C with cooling in still air at room temperature. This allowed us to obtain in the steel an initial ferritic-pearlitic structure with dominance of a lamellar form of cementite in the pearlite. After the normalizing, the samples were quenched from the austenitic range from 930°C in water (20°C) and then tempered for 30 min at 200, 300, 400, 500, 600, and 700°C. We studied the structure and determined the physical and mechanical properties of the steel after each variant of heat treatment (Tables 1 – 3).

Structure after accelerated cooling (quenching). The structure of the water-quenched steel is represented by differently oriented grains (colonies) surrounded by some excess ferrite (Fig. 3) located chiefly over the boundaries of the former austenite grains. The bainite consists of lathes of bainitic ferrite and thin layers of untransformed (retained) austenite arranged over its boundaries. The fine ferrite laths chiefly alternate in an ordered manner with austenite layers (Fig. 3). The mean width of the laths is about 400 nm; that of the austenite layers is about 40 nm. The content of the retained austenite does not exceed 1%. The x-ray diffraction analysis reflects only traces of the latter. The γ-phase is identifiable by microdiffraction analysis under transmission electron microscopy (Fig. 3*d*). It should be noted that the location of austenite in the form of films surrounding the laths of bainitic ferrite determines largely the properties of carbide-free bainite in low-carbon steels. To estimate the range of formation of such structures we quenched some samples of steel 08KhFA at a rate exceeding that of water cooling ($v_{cool} \approx 150$ K/sec in an aqueous solution of 16% NaCl; $t = -10$°C). It can be seen in Fig. 4 that the regularity of the

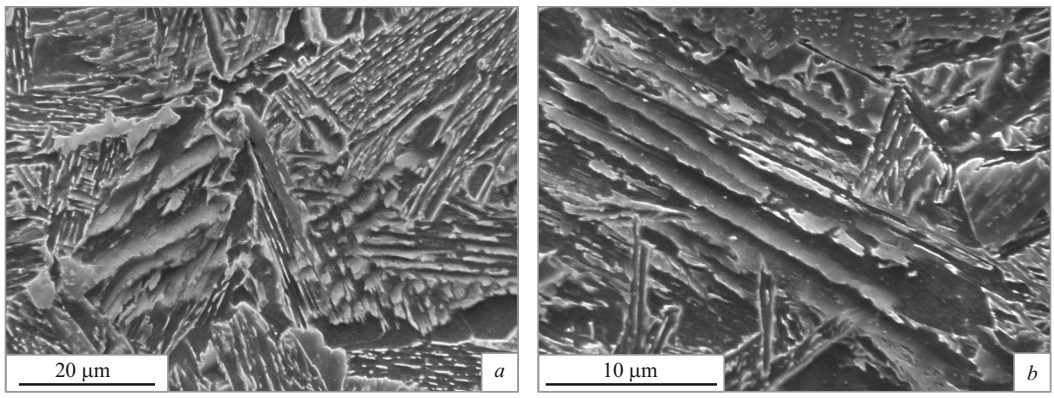

Fig. 4. Structure of steel 08KhFA (different magnifications) after quenching in a 16% aqueous solution of NaCl at – 10°C.

alternation of laths in the layers of the retained austenite does not change with decrease in the width of the ferrite laths).

Variation of structure and properties under tempering. The succession of the transformations of the structural state with elevation of the tempering temperature was studied by scanning electron microscopy (Fig. 5), transmission electron microscopy (Fig. 6) and x-ray diffraction analysis (Table 2). During tempering, the carbide-free lath bainite with excess ferrite over gain boundaries transforms progressively into a mixture of ferrite with globular carbide particles.

In the range of the tempering temperatures from 200 to 700°C, the mean grain size of about 10 μm remains virtually unchanged. Increase of the tempering temperature to 730°C, causes development of secondary recrystallization and abrupt grain growth (Fig. 5). The angles of misorientation of the grains grow as well as the fraction of the high-angle boundaries in the general distribution (Fig. 7), which elevates the ductility. It should be noted that the dislocation density after the quenching is quite high (5×10^{14} m^{-2}) and remains virtually unchanged up to the tempering temperature of 600°C (Table 1). Further increase of the tempering temperature and development of recrystallization processes produce marked lowering of the dislocation density. The third-kind residual stresses become progressively lower with increase of the tempering temperature (Table 1).

After the tempering at 200°C, retained austenite virtually disappears; at 300°C the structure acquires first precipitates of Fe_2C ε-carbide with an acicular shape (Fig. 6*a*). The microvolumes of the initial retained austenite are taken by ferrite with an enhanced dislocation density. Elevation of the tempering temperature to 400°C causes increase of the number of carbide particles inside the laths and appearance of single carbide precipitates on the boundaries of the former bainite laths. As a result of the tempering at 500°C, the content of carbide precipitates decreases, but their size and the degree of spheroidizing grow. Chains of round carbide inclusions appear on the boundaries of the former bainite laths (Fig. 6*c*). After the tempering at 600°C, the process of ferrite recrystallization is accelerated. The ferrite grains acquire a rounder shape. Spherical carbide precipitates are observable

TABLE 1. Residual Stresses of the Third Kind (σ_{resIII}), Dislocation Density (ρ), and Distribution of Carbon in Steel 08KhFA after Heat Treatment

Heat treatment	σ_{resIII}, MPa	$\rho \times 10^{14}$, m^{-2}	Distribution of carbon		
			In the volume		On dislocations
			$Q_{max}^{-1} \times 10^{-5}$	C, wt.%	$Q_{max}^{-1} \times 10^{-5}$
Quenching from 930°C	300	5.1	–	< 0.003	350
Quenching + tempering at 200°C	225	4.4	420	0.017	150
Quenching + tempering at 300°C	220	4.1	—	< 0.003	500
Quenching + tempering at 400°C	140	5.1	—	< 0.003	–
Quenching + tempering at 500°C	91	4.7	–	< 0.003	200
Quenching + tempering at 600°C	71	5.2	292	0.0117	1500
Quenching + tempering at 700°C	64	2.8	–	–	–
Normalizing at 940°C	130	2.0	–	–	–

Notations: Q_{max}^{-1}) maximum Snoek height in the volume of the sample and Snoek–Koster height on dislocations.

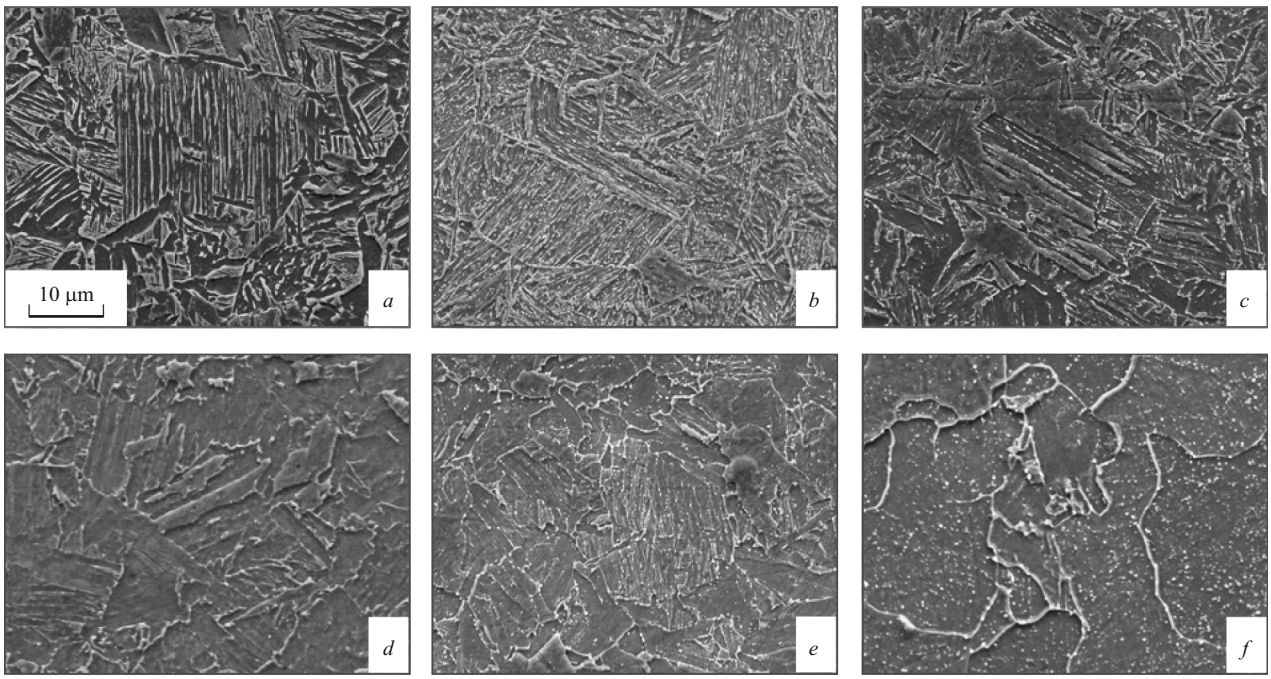

Fig. 5. Structure of steel 08KhFA (SEM) after quenching from 930°C and tempering at: *a*) 200°C; *b*) 400°C; *c*) 500°C; *d*) 600°C; *e*) 700°C; *f*) 730°C.

both inside the grains and on their boundaries. Above 700°C, the processes of secondary recrystallization develop intensely.

Distribution and condition of carbon. The main factors determining the mechanism and the kinetics of the processes of structural rearrangement are the mobility of the carbon atoms and the developing carbide reactions. We needed data on the quantitative distribution of carbon in the α-solid solution, retained austenite and carbides. To assess the concentration of carbon atoms in the bcc lattice in the regions of dislocation distortions, we used the method of internal friction. The temperature dependences of the internal friction and of the modulus of elasticity (Fig. 8) were measured in a device with a kilohertz frequency range for specimens with a size of 7 × 7 × 160 mm cut from the walls of a pipe over the rolling direction. The design of the device and the measurement technique are described in [11 – 13]. We studied the variation of the relaxation spectrum of the internal friction of steel 08KhFA upon increase of the tempering temperature.

Carbon steels are commonly characterized by appearance of Snoek and Snoek–Koster relaxation peaks on the temperature dependences of the internal friction. The Snoek peak is a result of residence of carbon atoms in the solid solution of the α-Fe lattice, and the Snoek–Koster peak is a result of residence of carbon atoms on dislocations. We used their heights in the temperature dependences of the internal friction of steel 08KhFA (Fig. 8) to assess the content of carbon atoms on the dislocations and in the volume (Table 1). The carbon concentration in the crystal lattice was calculated using the relation

$$C = KQ_{\max}^{-1}, \quad (1)$$

TABLE 2. Mechanical Properties of Steel 08KhFA after Tempering at Various Temperatures

Heat treatment	σ_r, MPa	$\sigma_{0.2}$, MPa	$\sigma_{0.2}/\sigma_r$	δ, %	KCV^{-50}, J/cm^2
Quenching from 930°C (initial state)	830	740	0.89	22.0	230
Quenching + tempering at 200°C	820	710	0.86	19.0	240
Quenching + tempering at 300°C	810	730	0.90	17.5	240
Quenching + tempering at 400°C	785	690	0.87	18.0	252
Quenching + tempering at 500°C	710	645	0.90	18.5	260
Quenching + tempering at 600°C	680	605	0.88	22.0	260
Quenching + tempering at 650°C	650	550	0.84	22.0	280
Quenching + tempering at 700°C	615	535	0.86	25.0	–
Quenching + tempering at 730°C	485	375	0.77	29.0	270

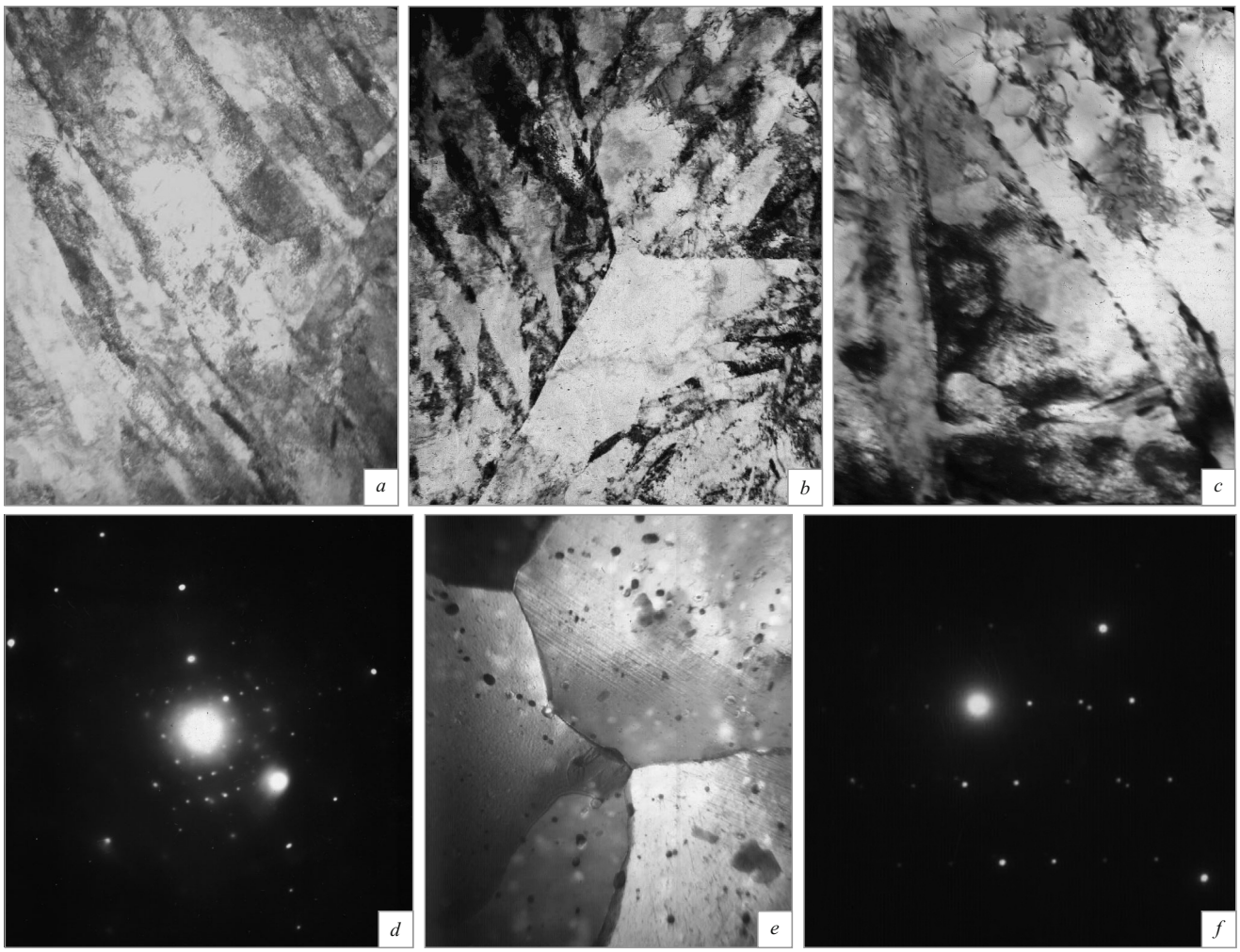

Fig. 6. Structure (*a*, *b*, *c*, *e*) and diffraction patterns (*d*, *f*) of steel 08KhFA (transmission electron microscopy) after quenching from 930°C and tempering at a temperature of: *a*) 300°C; *b*) 400°C; *c*, *d*) 500°C; *d*, *e*) 730°C; *a*, *b*) × 18000; *c*) × 24000; *d*) × 8000.

where K is a proportionality factor dependent on the grain size (for the grain size of 10 – 20 μm $K = 4$ [11]) and $Q_{\max}^{-1}$ is the height of the Snoek maximum. The minimum level of the assessment of the content of carbon from the Snoek peak is 0.003 wt.%, which can be seen from the data of Table 1.

We have not found a quantitative relation between the heights of the Snoek–Koster peaks and the concentration of the interstitial atoms on dislocations in the form of an analytical dependence. At the qualitative level, the appearance of a peak with a height $\geq 150 \times 10^{-5}$ relative unites indicates a considerable content of carbon atoms in the region of dislocations. It is obvious that the concentration of carbon in the defects of the solid solution of α-Fe, on dislocations in particular, will be higher than in the regions of undistorted lattice. After the tempering at up to 600°C, the dislocation density is preserved at a high level (about 5×10^{14} m^{-2}, Table 2), which determines the possibility of location of a considerable number of carbon atoms on dislocations. The structural changes occurring during the tempering at 200 and 600°C result in an abrupt growth of the concentration of carbon atoms in the volume of the crystal lattice of α-Fe (Table 1). In our opinion, this is explainable by transformation of the retained austenite into δ-ferrite (200°C) and by substitution of the cementite by special carbides (600°C).

Mechanical properties. We measured the mechanical properties of the steel after tempering at 200 – 730°C (Table 2). Though the microstructure of the steel undergoes some changes under tempering at 200 – 400°C, which are connected with carbon redistribution, precipitation of ε-carbide and decomposition of austenite layers, its mechanical characteristics (σ_r, $\sigma_{0.2}$ and δ) do not change considerably. At the same time, we may associate some decrease of δ after the tempering at 300°C with precipitation of ε-carbide. The most intense decrease in σ_r and $\sigma_{0.2}$ starts with the tempering at 600°C accompanied by polygonization and recrystallization of ferrite. Under the tempering above 730°C, the primary recrystallization is followed by secondary one and the grains coarsen (Fig. 5).

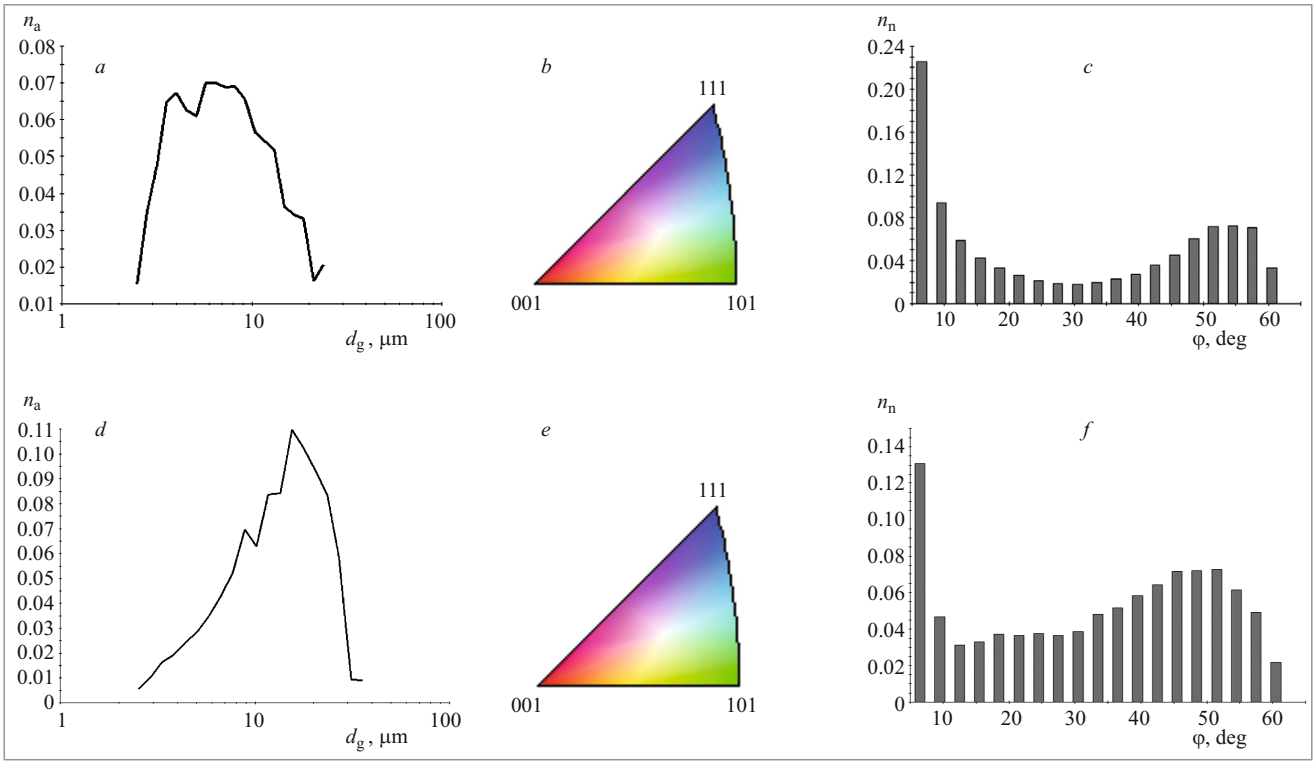

Fig. 7. Distribution of grains with respect to diameter d_g (a, d), misorientation angle φ of the grains (c, f), and stereographic triangles with color differentiation of the crystallographic directions (b, e) for steel 08KhFA after quenching from 930°C (a – c) and after quenching from 930°C and tempering at 700°C (b – f): n_a) fraction of grains with diameter d_g with respect to the area; n_n) fraction with respect to the total number of cases.

The ductility (δ_5) and the hardness (KCV^{-50}) of the quenched steel 08KhFA with a structure of carbide-free lath bainite with excess ferrite are quite high and remain virtually unchanged in tempering from 200 to 600°C (Table 2).

Corrosion resistance. Steel 08KhFA after quenching and tempering in the whole of the temperature range studied exhibits a relatively high resistance to hydrogen cracking and sulfide stress corrosion cracking (Table 3).

Somewhat unexpectedly, the considerable structural changes caused by the tempering at 200 – 700°C do not virtually affect the resistance of steel 08KhFA to carbon dioxide corrosion (Table 3, Fig. 9). Correctness of the values of the

TABLE 3. Corrosion Resistance of Steel 08KhFA after Tempering at Various Temperatures

Heat treatment	CRL, %	CTR, %	σ_{th}, % of σ_y	K_{Issc}, MPa · m$^{1/2}$	V_{CO_2}, mm/year
	I		II		III
Quenching from 930°C (initial state)	0	0	75	31.2	2.30
Quenching + tempering at 200°C	0	0	(668 h)	32.5	1.80
Quenching + tempering at 300°C	0	0	75	30.6	2.25
Quenching + tempering at 400°C	0	0	75	31.0	1.80
Quenching + tempering at 500°C	0	0	75	56.9	1.65
Quenching + tempering at 600°C	0	0	75	58.4	1.75
Quenching + tempering at 650°C	0	0	75	–	–
Quenching + tempering at 700°C	0	0	75	61.8	1.90
Quenching + tempering at 730°C	0	0	75	–	–

Notations: I) tests for hydrogen cracking; II) tests for sulfide stress corrosion cracking; III) tests for resistance to CO_2 corrosion.

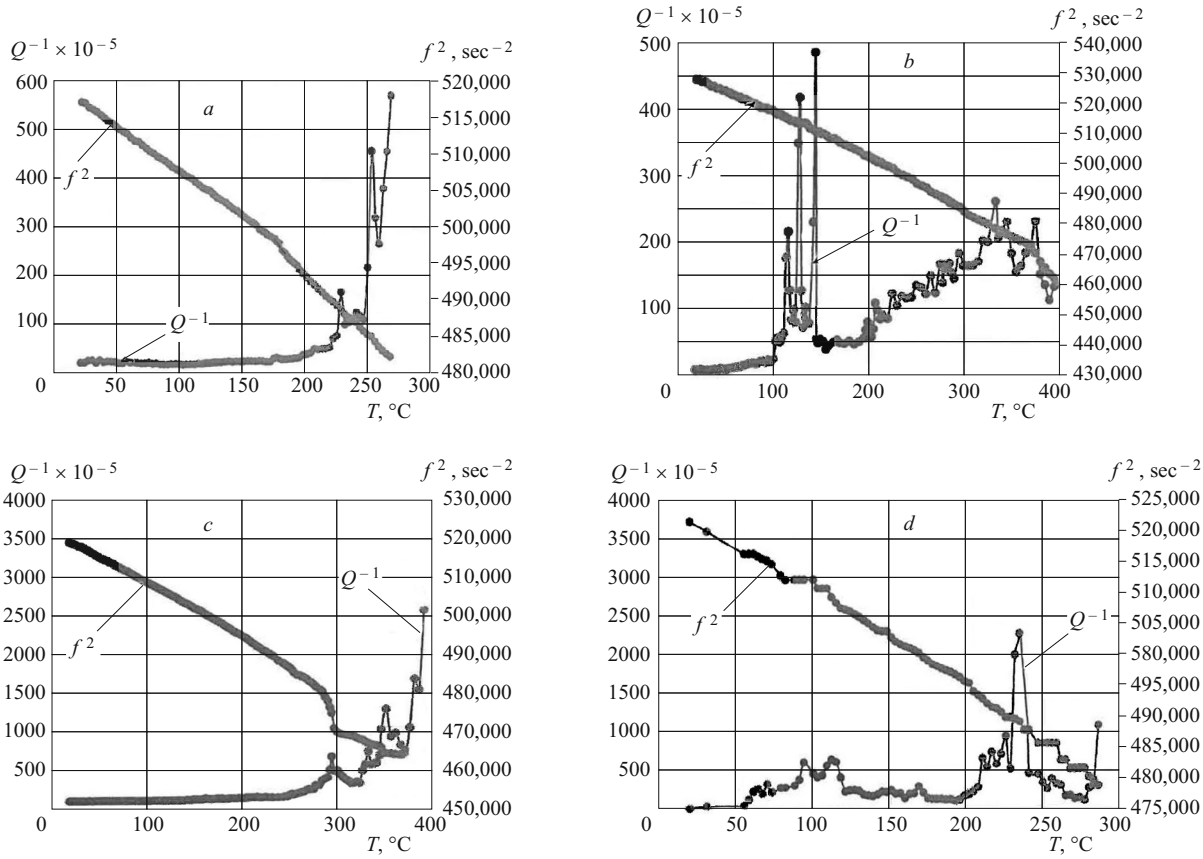

Fig. 8. Temperature dependences of internal friction Q^{-1} and of squared resonance frequency f^2 of steel 08KhFA after various treatment variants: *a*) quenching from 920°C; *b*, *c*, *d*) quenching from 920°C and tempering at 200, 400, and 600°C respectively.

rate of corrosion damage obtained is confirmed by closeness of the curves describing the variation of the concentration of Fe^{2+} in corrosion tests (Fig. 9*b*), which can be used for assessing the kinetics of the corrosion processes. According to reported data, the rate of corrosion of chromium-containing steels of type 08KhFA is determined by formation of a protective layer of chromium-enriched corrosion products on the surface. The protective layer is formed with participation of only the chromium contained in the solid solution but not in the carbides. The close values of corrosion rates at different tempering temperatures can be explained by the fact that the content of chromium in the solid solution of steel 08KhFA remains constant upon lowering of the carbon concentration.

DISCUSSION

The results obtained allow us to describe the succession of the changes in the structural state and properties of lath carbide-free bainite in low-carbon steels during tempering.

1. After quenching (the initial condition), carbon is located in lath carbide-free bainite in the layers of untransformed austenite and in the bainitic ferrite, concentrating on dislocations.

2. Tempering at 200°C causes decomposition of the layers of untransformed (retained) austenite, which follows from the data of the transmission electron microscopy, and marked increase of the carbon concentration in the bainitic ferrite.

As a rule, the decomposition of retained austenite is associated with higher temperatures. We have estimated the diffusion mobility of carbon and its migration from the untransformed austenite into the bainitic ferrite. The bainitic ferrite is characterized by a high dislocation density and presence of carbide pre-segregations. This is responsible for a higher solubility of carbon than in the equilibrium state and, consequently, for the appearance of a diffusion flow of carbon from the untransformed austenite.

The diffusion path of carbon atoms is calculated by the formula

$$X = 2\sqrt{D\tau}, \qquad (2)$$

where D is the diffusivity and τ is the tempering time.

At 200°C, $D = 10^{-12}$ cm^2/sec [14] and $\tau = 30$ min (1800 sec). Then $X = 8.5 \times 10^{-5}$ cm or 850 nm. This diffusion distance is 20 times longer than the mean width of the layers of untransformed austenite and 2 times longer than the

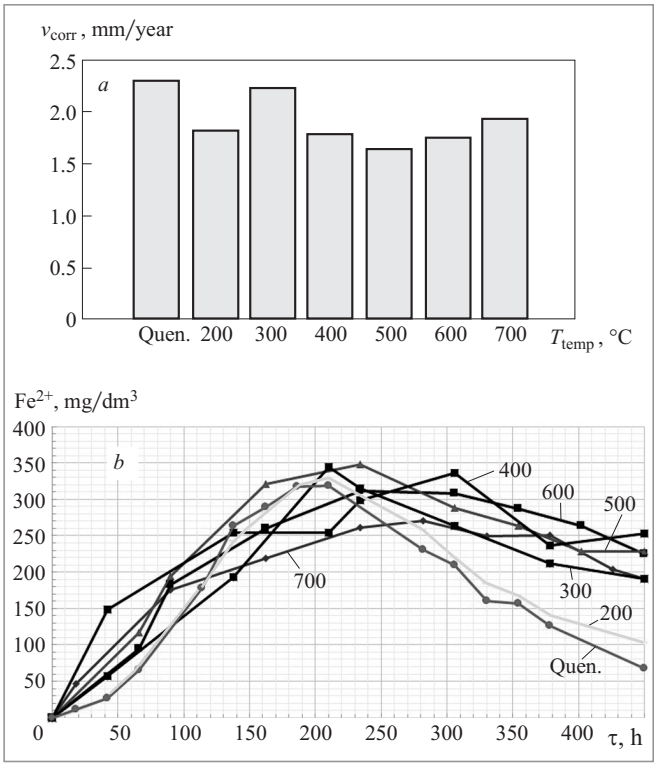

Fig. 9. Rate of carbon dioxide corrosion as a function of tempering temperature after quenching (Quen.) from 930°C (*a*) and of concentration of Fe^{2+} in the model environment as a function of the time of corrosion testing (*b*) of steel 08KhFA after tempering at various temperatures (given at the curves in °C).

average size of the bainite laths, which is quite enough for the diffusion removal of carbon from the layers of untransformed austenite.

Under actual conditions, carbon diffusion occurs in a nonequilibrium system (bainite – untransformed austenite) and depends on the hydrostatic stresses caused by the difference in the specific volumes of the austenitic and ferritic phases. The stability of untransformed austenite in the bainitic structures of low-carbon steels is considered in [15]. It is shown there that the maximum compressive stresses may attain 2320 MPa at a 0.04% volume fraction of untransformed austenite, and that austenite particles may be preserved up to the temperature of –77°C. We used the data of [15] (the modulus of elasticity of austenite E_{aust} = 160 GPa, the coefficient of the temperature expansion of ferrite 4.753×10^{-5} and that of austenite 6.991×10^{-5}) to estimate the stresses in the thin austenite layers. It turned out that the compressive stresses attained 960 MPa at the tempering temperature of 200°C. At this stress level and great length of the surrounding low-angle boundaries, the diffusion flow of carbon atoms from the region of compression (austenite) can exceed substantially the values reported for the equilibrium state. Accordingly, the diffusion mobility of carbon at 200°C can be enough for its migration from the thin austenite layers and development of a transformation of retained austenite into bainitic ferrite.

3. As a result of tempering at 300°C the structure acquires the first precipitates of acicular cementite.

4. Tempering at 400 – 500°C gives rise to polygonization processes and lowers the content of low-angle boundaries. The sizes of individual particles grow and they become spheroidized. Chains of carbide inclusions appear on the boundaries of bainite laths. The abrupt reduction of the third-kind residual stresses (Table 1) indicates transition of carbon from the crystal lattice into a bound condition in the form of carbides.

5. Tempering at 600°C produces intense development of recrystallization processes. Carbide reactions of substitution of cementite by special carbides start to develop. The concentration of carbon in the solid solution increases.

6. In tempering above 700°C, the primary recrystallization is accompanied by secondary one, and the sizes of the ferrite grains grow much.

CONCLUSIONS

1. Layers of untransformed austenite in the bainitic structure of steel 08KhFA decompose in low tempering (200°C). The mobility of carbon is responsible for the kinetics of this transformation.

2. The rate of carbon dioxide corrosion of quenched steel 08KhFA depends little on the temperature of the subsequent tempering (from 200 to 700°C) and on the occurring structural transformations.

3. The lath carbide-free bainite provides combination of high mechanical properties and corrosion resistance in low-carbon steels used in oilfield environments, which makes the expedience of their tempering questionable.

REFERENCES

1. V. V. Zav'yalov, *Problems of Operational Reliability of Pipelines in the Late Stage of Field Development* [in Russian], OAO "VNIIO-ENG," Moscow (2005), 322 p.
2. L. I. Efron, *Metal Science in "High" Metallurgy. Pipe Steels* [in Russian], Metallurgizdat, Moscow (2012), 696 p.
3. A. V. Ioffe, *Scientific Foundations of Development of Steels with Elevated Strength and Corrosion Resistance for the Production of Oilfield Pipes, Author's Abstract of Candidate's Thesis* [in Russian], Penza (2018), 362 p.
4. H. K. D. H. Bhadeshia, *Bainite in Steels*, Cambridge Press (2001), 479 p.
5. *Quantitative Structure–Property Relationships for Complex Bainitic Microstructures*, Commission of European Community ECSC. Sponsored Research Project, Swedish Inst. Metals Research, SIMR Report, IM-2004-247.07, 157 p.
6. A. V. Ioffe, "Creation of bainitic structures in the production of pipe steels," in: *Advanced Materials* [in Russian], Izd. TGU, Tolyatti (2017), Vol. VI, Ch. 3, pp. 153 – 196.
7. V. M. Schastlivtsev, Yu. V. Kaletina, E. A. Fokina, and A. Yu. Kaletin, "Effect of cooling rate on the content of retained

austenite under bainitic transformation," *Fiz. Met. Metalloved*., **115**(10), 1052 – 1063 (2014).
8. N. Yu. Zolotarevskii, A. A. Zisman, S. N. Panpurin, et al., "Effect of grain size and deformation structure of austenite on the crystal geometry features of bainite and martensite in low-carbon steels," *Metalloved. Term. Obrab. Met*., No. 10, 39 – 48 (2013).
9. A. R. Mishestyan, I. N. Shabalov, O. N. Chevskaya, and G. A. Filippov, "A study of the mechanism of variation of structural state in the process of deformation aging and its effect on the properties of pipe steel of bainitic type," *Chern. Metall., Byul*., No. 9, 77 – 92 (2018).
10. I. L. Yakovleva, N. A. Tereshchenko, and N. V. Urtsev, "Observation of the martensite-austenite component in the structure of low-carbon low-alloy pipe steel," *Fiz. Met. Metalloved*., **121**(4), 396 – 402 (2020).
11. M. S. Blanter, Yu. V. Piguzov, G. M. Ashchmarin, et al., *Method of Internal Friction in Metal Science Research* [in Russian], Metallurgiya, Moscow (1991), 248 p.
12. M. A. Vyboishchik, "Method of internal friction," in: *Advanced Materials. Structure and Methods of Research* [in Russian], Izd. TGU, Tolyatti (2006), Ch. 13, pp. 457 – 480.
13. M. S. Blanter, "Mechanical spectroscopy," in: *Advanced Materials* [in Russian], Izd. TGU, Tolyatti (2011), Vol. IV, Ch. 7, pp. 397 – 428.
14. B. S. Bokshtein, *Diffusion in Metals* [in Russian], Metallurgiya, Moscow (1978), 247 p.
15. N. G. Kolbasnikov, M. S. Sakharov, S. A. Kuzin, and V. S. Teteryatnikov, "About stability of untransformed austenite in the M/A phase of bainitic structure in low-carbon steel," *Metalloved. Term. Obrab. Met*., No. 2, 3 – 9 (2021).